

Novel Purine Nitrile Derived Inhibitors of the Cysteine Protease Cathepsin K

Eva Altmann,* Sandra W. Cowan-Jacob, and Martin Missbach*

Novartis Institutes for BioMedical Research,
CH-4002 Basel, Switzerland

Received August 20, 2004

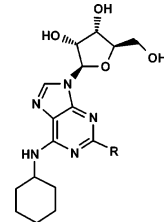
Abstract: Starting from the high-throughput screening hit **1a**, novel cathepsin K inhibitors have been developed based on a purine scaffold. High-resolution X-ray structures of several derivatives have revealed the binding mode of these unique cysteine protease inhibitors.

Cysteine proteases have received increasing interest as targets for therapeutic intervention in different disease areas. This has led to considerable efforts aimed at the discovery, design, and optimization of novel cysteine protease inhibitors.^{1–6} Cathepsin K is a lysosomal cysteine protease which is considered to be the key enzyme responsible for resorption of the bone matrix. Its ability to degrade type I collagen both within and outside the helical regions make it a unique mammalian protease.^{7–10} Deficiency in or inhibition of cathepsin K results in impaired activity of bone resorbing osteoclasts. In addition, mice lacking cathepsin K exhibit osteopetrosis, confirming the importance of this enzyme for bone remodeling.^{11,12} The crucial role cathepsin K plays in bone matrix resorption is further demonstrated by a rare human skeletal dysplasia, pycnodysostosis, which is the consequence of mutations in the cathepsin K gene.^{13–15} Thus, the development of specific inhibitors for this protease may offer an efficacious treatment for diseases characterized by excessive bone loss such as osteoporosis.

In this communication we report on a new class of highly potent heterocyclic inhibitors of cathepsin K. The starting point for our investigations of these inhibitors was the low-nanomolar high-throughput screening (HTS) hit **1a**. The compound is based on a purine template, which is an unprecedented scaffold for cysteine protease inhibition. Our first objective in the evaluation of this screening hit was to establish whether the nitrile group is the active principle of this inhibitor. As can be seen from Table 1, replacement of the 2-cyano moiety in **1a** by a methyl or hydroxymethyl substituent, as in **1b** and **1c**, respectively, is detrimental to inhibition, thus demonstrating the crucial role of this group. These initial findings indicate that cathepsin K inhibition by **1a** probably involves covalent interaction of the nitrile carbon with the active site Cys-25 sulfhydryl group.

To convert the HTS hit **1a** into a truly viable lead, replacement of the ribose moiety was an essential prerequisite. On the basis of molecular modeling studies and prior experience with other classes of cathepsin K inhibitors, we hypothesized that the 6-aminocyclohexyl

Table 1. Compounds **1a–c** Profiling Data



compd	R	IC ₅₀ (μM) ^a		
		Cath K	Cath L	Cath S
1a	CN	0.014	0.430	0.340
1b	CH ₃	≥1	>10	>10
1c	CH ₂ OH	≥1	>10	>10

^a Inhibition of rh cathepsins K, L, and S in a fluorescence-based assay employing Z-Phe-Arg-AMC (cathepsins K and L) and Z-Leu-Leu-Arg-AMC (cathepsin S) as synthetic substrates. Data represent the mean of two experiments performed in duplicate.

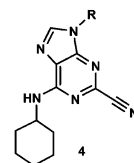


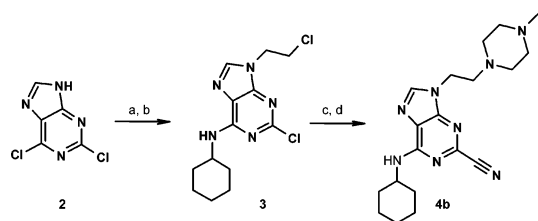
Figure 1.

ring of **1a** was likely to bind in the lipophilic S2 subsite of the enzyme while the sugar moiety would reach toward the surface of the enzyme. On the basis of this assumption, a series of purine-derived compounds **4** (Figure 1) incorporating hydrophilic R groups were prepared. As a representative example, the synthesis of **4b** is outlined in Scheme 1. Thus, commercially available 2,6-dichloropurine (**2**) was reacted with cyclohexylamine to afford the 6-aminocyclohexyl-substituted purine derivative which was then converted into **3** by treatment with 1-chloro-2-bromoethane. Subsequent reaction of **3** with 1-methylpiperazine followed by the displacement of the 2-chloro substituent with cyanide furnished the target molecule **4b**.

As summarized in Table 2 substitution of the sugar moiety in **1a** by a simple cyclopentane ring led to the highly potent inhibitor **4a**, which also showed significant selectivity over inhibition of cathepsins L and S. Replacement of the ribose moiety by a 4-methylpiperazinylethyl or by the linear (2-methoxyethyl)methylaminoethyl moiety likewise resulted in low nanomolar cathepsin K inhibitors **4b** and **4c**, respectively. However, compared to **4a** and **4b**, **4c** exhibits only moderate selectivity vs the highly homologous cathepsins L and S.

A high-resolution X-ray crystal structure of inhibitor **4b** bound in the active site of cathepsin K (Figure 2) confirmed the predicted binding mode for these purine derivatives. As expected, **4b** is found to bind covalently to the S_γ of active site Cys-25, the resulting thioimidate moiety being coplanar with the central part of the inhibitor. The purine scaffold packs against the hydrophobic wall of the cathepsin K active site, while the cyclohexyl group is the P2 moiety and occupies the

* To whom correspondence should be addressed. For E.A.: phone, +41 61 696 1227; fax, +41 61 696 6071; e-mail, eva.altmann@pharma.novartis.com. For M.M.: phone, +41 61 696 3962; fax, +41 61 696 6071; e-mail, martin.missbach@pharma.novartis.com.

Scheme 1^a

^a Reagents: (a) cyclohexylamine, pentan-1-ol, 70 °C, 4 h, 76%; (b) 1-chloro-2-bromoethane, K₂CO₃, DMF, 45 °C, 5 h, 53%; (c) 1-methylpiperazine, 50 °C, 7 h, 81%; (d) NaCN, DMA, 160 °C, 20 h, 26%.

Table 2. Selectivity Data on the Inhibition of Homologous Cathepsins

Compd	R	IC ₅₀ [nM] ^a		
		Cat K	Cat L	Cath S
4a		< 3	300	63
4b		6	89	150
4c		10	76	200

^a Inhibition of rh cathepsins K, L, and S in a fluorescence-based assay employing Z-Phe-Arg-AMC (cathepsins K and L) and Z-Leu-Leu-Arg-AMC (cathepsin S) as synthetic substrates. Data represent the mean of two experiments performed in duplicate.

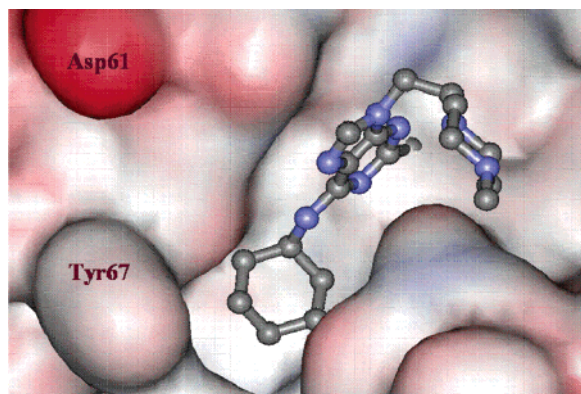


Figure 2. Purine **4b** cocrystallized in the cathepsin K active site. PDB code is 1U9V. Image was produced using Weblab-Viewer Lite (Accelrys, Inc.).

lyophobic S2 subsite. No direct interactions with the binding site are observed for the piperazinyl moiety.

On the basis of the above inhibition and structural data, we expanded our chemistry efforts to synthesize compounds that not only extend into the S2 pocket but in addition would have the potential to interact with amino acid residues of the S3 subsite. Because the S3 subsites show different characteristics between cathepsins K, S, and L, we hypothesized that this strategy would result in better compound selectivity through additional interaction points provided by a P3 residue. Modeling studies suggested two possibilities to reach the S3 subsite: namely either the addition of a substituent in the 2-position of the aminocyclohexyl group (which raises stereochemical issues); or the replacement of the cyclohexyl moiety by an ortho-substituted phenyl ring (Figure 3). Aspiring for achiral inhibitors **9a–d**

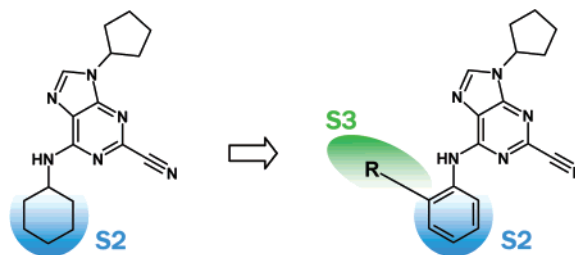
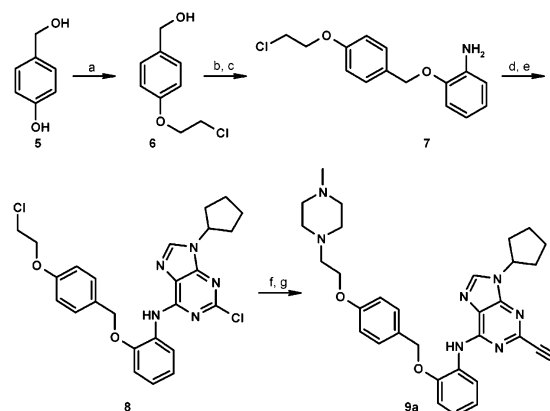


Figure 3. Potential expansion of purine derivatives **4** into S3.

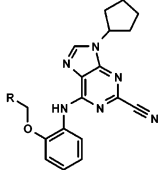
Scheme 2^a

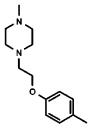
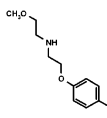
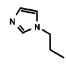
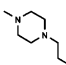
^a Reagents: (a) 1-chloro-2-bromoethane, K₂CO₃, KI, TBAB, acetone, 50 °C, 24 h, 41%; (b) 2-nitrophenol, DEAD, Ph₃P, THF, room temp, 4 h, 63%; (c) H₂, PtO₂, AcOEt, 3 h, 90%; (d) 2,6-dichloropurine, pentan-1-ol, 80 °C, 5 h, 56%; (e) bromocyclopentane, K₂CO₃, DMF, 50 °C, 60%; (f) 1-methylpiperazine, 50 °C, 2 h, 21%; (g) NaCN, DMA, 20 h, 150 °C, 56%.

incorporating an ortho-substituted phenyl ring were prepared. However, it should be emphasized that modeling also indicated the potential for other orientations of substituents attached to the 2-position of the phenyl ring that would not involve interactions with the S3 pocket and therefore would not lead to enhanced specificity. To distinguish these possibilities, we synthesized and investigated compounds **9**.

The preparation of compounds **9**, exemplified by **9a**, is outlined in Scheme 2. O-Alkylation of 4-hydroxymethylphenol **5** with 1-chloro-2-bromoethane afforded the benzyl alcohol **6**. This intermediate was reacted with 2-nitrophenol under Mitsunobu conditions, followed by reduction of the resulting nitro-phenyl-benzyl-ether with platinum oxide to yield the corresponding chloro-ethoxy-benzyloxy-phenylamine **7**. Elaboration to produce the 9-cyclopentyl-6-phenylaminopurine derivative **8** was achieved by reaction of **7** with 2,6-dichloropurine and subsequent alkylation of the 9-position of the purine nucleus with bromocyclopentane. Treatment of intermediate **8** with 1-methylpiperazine followed by the displacement of the 2-chloro substituent with cyanide provided the desired target molecule **9a**.

Initially we explored a para-substituted benzyloxy and a substituted propoxy moiety attached to the 2-position of the aminophenyl group. While the aryl part of the benzyloxy derivatives **9a** and **9b** was intended to interact with the phenyl ring of Tyr67 and thus improve the inhibitory activity and selectivity, the polar extension in the para position served to improve aqueous solubility. In contrast, the polar groups attached to the purine scaffold by a propoxy linker, as in **9c** and **9d**,

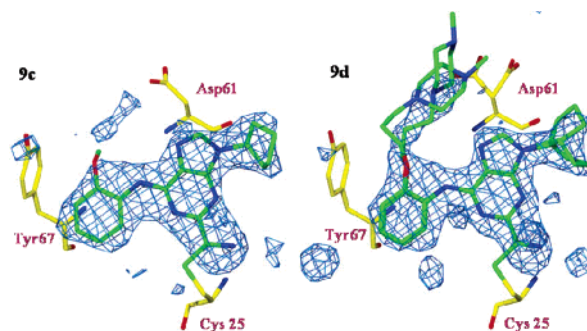
Table 3. Selectivity Data on the Inhibition of Homologous Cathepsins


Compd	R	IC ₅₀ [nM] ^a		
		Cat K	Cat L	Cat S
9a		26	560	50
9b		14	230	71
9c		3.5	44	210
9d		7	82	260

^a Inhibition of rh cathepsins K, L, and S in a fluorescence-based assay employing Z-Phe-Arg-AMC (cath K and L) and Z-Leu-Leu-Arg-AMC (cath S) as synthetic substrates. Data represent the mean of two experiments performed in duplicate.

were also meant to interact with the side chain of Asp 61, thereby further improving activity and specificity for cathepsin K. The results displayed in Table 3 show that **9a–d** are generally low-nanomolar inhibitors of cathepsin K but do not exhibit improved potency compared to compounds **4**. Inhibitors **9a** and **9b** having a 2-benzyloxy substituent at the phenyl moiety are slightly less potent than **9c** and **9d**, which incorporate an *o*-propoxy linker positioned at the 6-aminophenyl ring. The observation that compounds **9** do not show a better overall specificity profile than compounds **4** indicated that the substituents attached to the 2-position of the aminophenyl moiety apparently do not extend into the S3 subsite of cathepsin K. However, it is noteworthy that the selectivity profile of compounds **9** changes depending on the nature of the spacer used to direct these potential P3 substituents into the S3 pocket. While 2-benzyloxy-containing compounds **9a** and **9b** have better selectivity vs cathepsin L, compounds with a 2-propoxy substituent, **9c** and **9d**, prove to be more specific against cathepsin S. In the functional in vitro rabbit bone-resorption assay, **9d** inhibits bone resorption with an IC₅₀ of 176 nM.¹⁶

X-ray crystal structures were obtained for complexes of **9c** and **9d** and cathepsin K. These structures revealed that the substituents that were intended to bind in the S3 subsite of the enzyme do not occupy a fixed position and face toward the solvent rather than bind in the S3 part of the active site cleft. The difference electron density map for **9c** (Figure 4 left) shows very strong contributions from the ligand except for the imidazolyl group and its propyl linker, indicating that this part of the molecule is highly flexible. The density for the cyclopentane ring also suggests that this group is in more than one orientation. The phenyl ring binds in the S2 subsite as expected. Interestingly the tilt of the

**Figure 4.** Difference electron density maps contoured at 2.5 σ of purine derivatives **9c** and **9d** (green) in complex with cathepsin K (yellow). PDB codes are 1U9W (**9c**) and 1U9X (**9d**). The picture was produced using the program O.¹⁷

purine ring in the active site cleft is slightly different from that observed in the X-ray structure of the cyclohexyl derivative **4b**/enzyme complex. In the case of **4b**, this tilt is necessary to enable the bulkier cyclohexyl moiety to fit into S2. Again, the nitrile forms a covalent bond to Cys25 of cathepsin K. The difference electron density map for the **9d**/cathepsin K complex is very similar to that of **9c** except that there is some weak density present for the propylpiperazine part of the inhibitor. This density was found to be best represented when two conformations were modeled. Multiple conformations were also modeled for the cyclopentane ring.

In summary, we have discovered novel potent cathepsin K inhibitors, starting from the purine-based HTS hit **1a**. A representative inhibitor (**9d**) of this purine series proved efficacious in a functional in vitro bone-resorption assay. Moreover, the high-resolution X-ray structure of **4b** was in good agreement with the predicted binding mode of these heterocyclic inhibitors and provides valuable information for the design of different nonpeptidic inhibitors.

Acknowledgment. The authors thank P. Ramage, S. Geisse, and T. Inaoka for cathepsin K production,¹⁸ S. Niwa for performing the bone-resorption assay, and I. Sigg for technical assistance.

Supporting Information Available: Description of the inhibition assays and characterization (¹H NMR and HRMS) of **1a–c**, **4a–c**, and **9a–d** and crystallographic structure determination of **4b**, **9c**, and **9d** in complex with cathepsin K. This material is available free of charge via the Internet at <http://pubs.acs.org>.

References

- Hernandez, A. A.; Roush, W. R. Recent advances in the synthesis, design and selection of cysteine protease inhibitors. *Curr Opin. Chem. Biol.* **2002**, *6*, 45–465.
- Leung, D.; Abbenante, G.; Fairlie, D. P. Protease inhibitors: current status and future prospects. *J. Med. Chem.* **2000**, *43*, 305–341.
- Yamashita, D. S.; Dodds, R. A. Cathepsin K and the design of inhibitors of cathepsin K. *Curr. Pharm. Des.* **2000**, *6*, 1–24.
- Veber, D. F.; Thompson, S. K. The therapeutic potential of advances in cysteine protease inhibitor design. *Curr. Opin. Drug Discovery Dev.* **2000**, *3*, 362–369.
- Marquis, R. W. Inhibition of cysteine proteases. *Annu. Rep. Med. Chem.* **2000**, *35*, 309–320.
- Deaton, D. N.; Kumar, S. Cathepsin K inhibitors: their potential as anti-osteoporosis agents. *Prog. Med. Chem.* **2004**, *42*, 245–375.
- Inaoka, T.; Bilbe, G.; Ishibashi, O.; Tezuka, K.; Kumegawa, M.; Kokubo, T. Molecular cloning of human c-DNA for cathepsin K: novel cysteine protease predominantly expressed in bone. *Biochem. Biophys. Res. Commun.* **1995**, *206*, 89–96.

- (8) Drake, F. H.; Dodds, R. A.; James, I. E.; Connor, J. R.; Debouck, C.; Richardson, S.; Lee-Rykaczewski, E.; Coleman, L.; Rieman, D.; Bathlow, R.; Hastings, G.; Gowen, M. Cathepsin K but not cathepsins B, L, or S is abundantly expressed in human osteoclasts. *J. Biol. Chem.* **1996**, *271*, 12511–12516.
- (9) Bossard, M. J.; Tomaszek, T. A.; Thompson, S. K.; Amegadzie, B. Y.; Hanning, C. R.; Jones, C.; Kurdyla, J. T.; McNulty, D. E.; Drake, F. H.; Gowen, M.; Levy, M. A. Proteolytic activity of human osteoclast cathepsin K. Expression, purification, activation and substrate identification. *J. Biol. Chem.* **1996**, *271*, 12517–12524.
- (10) Garnero, P.; Borel, O.; Byrjalsen, I.; Ferreras, M.; Drake, F. H.; McQueney, M. S.; Foged, N. T.; Delmas, P. D.; Delaisse, J.-M. The collagenolytic activity of cathepsin K is unique among mammalian proteinases. *J. Biol. Chem.* **1998**, *273*, 32347–32352.
- (11) Saftig, P.; Hunziker, E.; Wehmeyer, O.; Jones, S.; Boyde, A.; Rommerskirch, W.; Moritz, J. D.; Schu, P.; von Figura, K. Impaired osteoclastic bone resorption leads to osteopetrosis in cathepsin-K-deficient mice. *Proc. Natl. Acad. Sci. U.S.A.* **1998**, *95*, 13453–13458.
- (12) Gowen, M.; Lazner, F.; Dodds, R.; Kapadia, R.; Feild, J.; Tavarina, M.; Bertonecello, I.; Drake, F.; Zavorselk, S.; Tellis, I.; Hertzog, P.; Debouck, C.; Kola, I. Cathepsin K knockout mice develop osteopetrosis due to a deficit in matrix degradation but not demineralization. *J. Bone Miner. Res.* **1999**, *14*, 1654–1663.
- (13) Gelb, B. D.; Edelson, J. G.; Desnick, R. J. Linkage of pycnodysostosis to chromosome 1q21 by homozygosity mapping. *Nat. Genet.* **1995**, *10*, 235–237.
- (14) Polymeropoulos, M. H.; Ortiz De Luna, R. I.; Ide, S. E.; Torres, R.; Rubenstein, J.; Francomano, C. A. The gene for pycnodysostosis maps to human chromosome 1cen-q121. *Nat. Genet.* **1995**, *10*, 238–239.
- (15) Hou, W. S.; Brömme, D.; Zhao, Y.; Mehler, E.; Dushey, C.; Weinstein, H.; Miranda, C. S.; Fraga, C.; Greig, F.; Carey, J.; Rimon, D. L.; Desnick, R. J.; Gelb, B. D. Characterization of novel cathepsin K mutations in the pro and mature polypeptide regions causing pycnodysostosis. *J. Clin. Invest.* **1999**, *103*, 731–738.
- (16) Kakudo, S.; Miyazawa, K.; Mano, H.; Mori, Y.; Yuasa, T.; Nakamaru, Y.; Shiokawa, M.; Nagahira, K.; Tokunaga, S.; Hakeda, Y.; Kumegawa, M. Isolation of highly enriched rabbit osteoclasts from collagen gels: A new assay system for bone resorbing activity of mature osteoclasts. *J. Bone Miner. Metab.* **1996**, *14*, 129–136.
- (17) Jones, T. A.; Zou, J.-Y.; Cowan, S. W., Kjeldgaard, M. Improved methods for building protein models into electron density maps and the location of errors in these models. *Acta Crystallogr.* **1991**, *A47*, 110–119.
- (18) Manuscript on cathepsin K production is in preparation.

JM0493111